NMR-Based metabolomic analysis of the anticancer effect of metformin on cholangiocarcinoma cells

Jin Zhang (zj52811227@live.com)
Xiamen University https://orcid.org/0000-0001-8695-5112
Caihua Hang
Xiamen University of Technology
Wei Shao
Xiamen University Affiliated Chenggong Hospital
Wengang Li
Xiamen University
Donghai Lin
Xiamen University

Research article

Keywords: cholangiocarcinoma, NMR-based metabolomic analysis, metformin

Posted Date: January 29th, 2020

DOI: https://doi.org/10.21203/rs.2.22216/v1

Version of Record: A version of this preprint was published at Frontiers in Oncology on November 30th, 2023. See the published version at https://doi.org/10.3389/fonc.2020.570516.

Abstract

Background Metformin is a widely prescribed anti-diabetes drug with potential utilities for cancer therapies. Several previous studies have related metformin to the reduced risk of cholangiocarcinoma (CCA), highlighting its potentialities for the treatments of CCA.

Methods In this study, cell viability assay and colony formation assay were used to test the inhibition effect of metformin on Mz-ChA-1 cells. The NMR-based metabonomic analysis was conduct to compare the differences between the metformin-treated (Met) and control (Ctrl) groups of the Mz-ChA-1 cells. Significant metabolites were identified from multivariate statistical analysis of 1D 1 H-NMR spectral data, and differential metabolites were identified from the pair-wise t-test of the metabolite levels. Significantly altered metabolic pathways were identified based on characteristic metabolites which were determined by a combination of the significant metabolites and differential metabolites.

Results Here, we demonstrated that metformin treatment could inhibit the proliferation of the CCA cell line Mz-ChA-1 in a dose-dependent manner. The NMR-based metabonomic analysis showed a distinct discrimination between the Met and Ctrl groups of the Mz-ChA-1 cells. Moreover, The Met group exhibited promoted glycolysis and suppressed TCA cycle compared with the Ctrl group. While metformin treatment decreased non-essential amino acids, it also increased essential amino acids and UDP-GlcNAc, implying the occurrence of autophagy and cell cycle arrest in metformin-treated CAA cells .

Conclusions This work provides a mechanistic understanding of the anticancer effect of metformin on CAA, and is beneficial to the further development of metformin as an anticancer drug

Background

Cholangiocarcinoma (CCA) is the second most common hepatic and biliary malignancy [1]. Based on its anatomical location, CCA can be classified into intrahepatic, extrahepatic and distal CCA [1, 2]. Although CCA is considered as an uncommon tumor and only accounts for 3% of all gastrointestinal tumors, the overall incidence rate of CCA has remarkably climbed in last several decades [3, 4]. Surgical intervention offers the highest chance to cure for all types of CCA. Unfortunately, individuals with CCA are usually asymptomatic, and most of patients diagnosed with CCA can no longer benefit from surgical resection [4], leading to poor outcomes. Even when surgery is an option for selected patients, the 5-year survival rates are still very low. Both systemic chemotherapy and targeted radiation therapy have been also applied for the treatments of CCA. Nevertheless, these approaches are usually failed to greatly improve the prognosis of CCA [3]. Thus, new therapy strategies are urgently needed for CCA.

As the most widely used first-line drug for the treatment of type 2 diabetes, metformin (N, N-dimethylbiguanide) has recently gained increasing interests of investigators for its anticancer potentials. According to recent epidemiological data, cancer risk in diabetic patients taking metformin is reduced relative to patients with other antidiabetic treatments [5–8]. Moreover, numerous studies have reported that metformin has anticancer effects both in vivo and in vitro on various human cancers including CCA

[9–13]. These evidences indicate that metformin might have great potentials for CCA prevention and therapy.

Recently it was showed that metformin reduced the levels of mitochondrial metabolites, activated multiple mitochondrial metabolic pathways, and increased 18-FDG flux in breast tumors [14]. Moreover, metformin could inhibit mitochondrial complex I and disrupt the oxidative phosphorylation, then resulting in alterations in the electron transport chain (ETC) [15, 16]. Inhibition of complex I also caused energetic stress, and thus enhanced the activity of AMP-activated protein kinase (AMPK) [17, 18]. Furthermore, metformin could activate AMPK through the lysosomal pathway, and the anticancer effect of metformin might be not mere a consequence of disrupting metabolic processes such as ATP synthesis through oxidation phosphorylation [19]. In addition, previous works also indicated that metformin exerted anticancer capacities by inhibiting the mammalian target of rapamycin (mTOR) through AMPK-dependent and AMPK-independent mechanisms [20, 21]. However, molecular mechanisms under the anticancer effect of metformin on CCA remain to be detailedly clarified.

Metabolomic analysis has been extensively applied to clarify molecular mechanisms of anticancer drugs [22–24]. As metabolites are the final downstream products of gene transcription and translation, variations in metabolite levels reflect systemic changes of biological states. Several complicated signaling pathways could simultaneously bring out alterations in a metabolic pathway. Therefore, a comprehensive metabolomic analysis is of great significance for elucidating the molecular mechanisms of metformin for the treatments of CAA.

In the present work, we demonstrated that metformin treatment profoundly suppressed the proliferation of CCA cell line MZ-CHA–1 in a dose-dependent manner. By performing a NMR-based metabonomic analysis, we indicated that metformin induced marked variations of metabolic profiles and remarkable changes of metabolite levels as well as significant alterations in metabolic pathways. These results may shed light on the anticancer effect of metformin on CAA.

Materials and Methods

Cell lines and culture

The human cholangiocarcinoma cancer cell line MZ-CHA–1 was originally established from mechanically dissociated gallbladder metastases of adenocarcinoma of the extrahepatic biliary tract [25] and was conserved in our laboratory. Cells were cultured in RPMI 1640 supplemented with 10% fetal bovine serum (FBS, Gemini, USA).

Cell viability assay

The cell viability assay was performed on Mz-ChA–1 cellsusing a CellTiter 96®AQueous One Solution Cell Proliferation Assay Kit (Promega, USA) according to the recommendations of the manufacturer. Cells

were seeded in 96-well plates (5×10^3 per well). After 12 h, medium was replaced with test medium containing various concentrations of metformin (0.05, 0.5, 2, 5 mM), and the cells were incubated for further 48 h. Then, 20 μl of MTS solution was added to each well. After 4 h incubation in dark, the absorbance of formazan was measured at a wavelength of 490 nm on a microplate reader (BioTek, USA). Results are presented as the mean ± SEM. Data were analyzed by pairwise t-test to compare cell viabilities between the four metformin-treated (Met) groups and the control (Ctrl) group using GraphPad Prism (version 6, GraphPad Software, USA).

Colony formation assay

Cells were planted into 6-well plates at a density of 1000 cells per well, and treated with test medium containing various concentrations of metformin for 7–14 d. Colonies were fixed with 4% paraformaldehyde for 20 min, and stained with 0.5% crystal violet in 20% ethanol for 30 min. The plates were washed with water for 3 times and photographed with camera.

Samples preparation

Cells were seeded in 10-cm diameter culture dishes at a density of 1×10^6 per dish and treated with or without 0.5 mM metformin for 48 h. Before harvest, medium was removed and cells were quickly washed by ice-cold PBS for 3 times. Vacuum suction was used to remove any residual liquid. Next, 3.0 ml of cold methanol was immediately added into the culture dish, and the cells were scraped, collected and transferred into a centrifuge tube. Then, 3.0 ml of cold chloroform and 2.5 ml of water were subsequently added to the tube, and the mixture was fully vortexed. After 30 min of laying aside, samples were centrifuged at 12 000 g for 15 min at 4 ℃ to separate two phase extracts. Aqueous phase was condensed with nitrogen stream and lyophilized by a vacuum freezing dryer.

Lyophilized aqueous intracellular metabolite extracts were dissolved in 550 μl of NMR buffer containing 50 mM K_2HPO_4/NaH_2PO_4 (pH 7.4), 0.05 mM sodium 3-(trimethylsilyl)-propionate–2,2,3,3-d4 (TSP), 10% D_2O and 0.02% NaN_3. D_2O was used for a field-frequency lock, and TSP provided the chemical shift reference. All the samples were vortexed, centrifuged at 12000 g for 15 min at 4 °C to remove any insoluble components. Supernatants were transferred to 5-mm NMR tubes for further analysis.

NMR measurements and data processing

NMR experiments were conducted on a Bruker Avance III 850MHz spectrometer (Bruker BioSpin, Rheinstetten, Germany) at 298 K. One dimensional (1D) ^{1}H NOESY spectra were acquired using the pulse sequence [(RD)–90°-t1–90°-τ_m–90°-ACQ] with water suppression during the relaxation delay and mixing time (19). RD was the relaxation delay (4 s), t1 was a short delay (4μs), and τ_m was the mixing time (10 ms). The spectral width was 20 ppm with an acquisition time per scan of 1.88 s, and a total of 128

transients were collected into 64 K data points for each spectrum. Chemical shifts were referenced to the methyl-group of TSP at 0 ppm. Phase corrections, baseline corrections and spectra alignment were manually conducted using MestReNova Version 9.0 (Mestrelab Research S. L., Espain). Spectral regions of δ 9.40-(−0.5) were binned by 0.001 ppm and integrals of the segments were calculated. Regions of residual water resonances at δ 5.2–4.6 were removed to eliminate the distorted baselines from imperfect water saturation.

Integrals were normalized by the integral area of TSP to make the data directly comparable between the spectra. Then, probabilistic quotient normalization (PQN) was performed to compensate for dilution-independent effects in MATLAB (Version 2011b, Math Works, USA).

Multivariate statistical analysis and identification of significant metabolites

The normalized spectral data were scaled by Pareto scaling and objected to the SIMCA-P+12.0 software (Umetrics, Sweden) for multivariate statistical analysis. An unsupervised approach, principal component analysis (PCA) was performed to reveal the trends, highlight outliers, and show clusters among the samples. A supervised approach, partial least-squares discriminant analysis (PLS-DA) was subsequently conducted to improve the classification between the groups of the samples. Cross-validation by a random permutation test (999 cycles) was performed to evaluate the robustness of the PLS-DA model. The model is considered credible if all the Q2-values on the left are lower than the original point at the right, and the regression line of the Q2-points intersects the vertical axis below zero.Two criterions derived from the PLS-DA loading plot were used to identify significant metabolites primarily responsible for the metabolic discrimination: variable importance in the projection (VIP), and the correlation coefficient (r) of the variable relative to the first predictive component (tp1). The loading plot was reconstituted in MATLAB. The critical value of correlation coefficient (r) was defined based on the degree of freedom (df), which were determined as n1+n2−2 with n1 and n2 as the respective number of samples of the two groups in the PLS-DA model. Variables with VIP > 1 and |r| > the critical value of p = 0.01 were marked by red color; variables with VIP > 1 and |r| between the critical values of p = 0.05 and p = 0.01 were marked by orange; variables with VIP ≤ 1 or |r| < the critical value of p = 0.05 were marked by blue. Variables colored in red and orange were related to significant metabolites.

Furthermore, hierarchical cluster analysis (HCA) with Pearson distance measure and Ward clustering algorithm was performed on the normalized NMR data to further confirm the metabolic clusters, using the module of Statistical Analysis provided by the MetaboAnalyst webserver 4.0 (http://www.metaboanalyst.ca/). In the HCA approach, each sample acted as a separate cluster initially and the algorithm proceeded to combine them until all samples belong to one cluster.

Resonance assignments and identification of differential metabolites

Resonance assignments of identified metabolites were conducted using a combination of Chenomx NMR Suite (version 8.1, Chenomx Inc., Edmonton, Canada) and Human Metabolome Data Base (HMDB) (http://www.hmdb.ca/) as well as relevant published references. For metabolites with highly overlapping peaks, only non-overlapping peaks were chosen to accurately calculate the relative concentrations of these metabolites, which were represented with the sums of the corresponding characteristic peak integrals. GraphPad Prism was used to calculate the averages and standard errors of metabolite concentrations. Student's t-test was applied to quantitatively compare relative concentrations of metabolites between the Met and Ctrl groups. Metabolites with p <0.05 were identified to be differential metabolites. Characteristic metabolites were identified by a combination of the significant metabolites and differential metabolites.

Metabolic pathway analysis and identification of significant pathways

Significantly disturbed metabolic pathways were identified based on the characteristic metabolites using the module of Metabolites Set Enrichment Analysis (MSEA) provided by MetaboAnalyst 4.0. MSEA is extensively used to identify and interpret patterns of metabolite concentration changes in a meaningful context [26]. The used metabolite set library in MSEA contains 88 metabolite sets, which correlates a group of functionally related metabolites to a metabolic pathway with enriched metabolites. The statistical p value was calculated to evaluate the significance of the metabolic pathway. The metabolic pathway containing at least three enriched metabolites with $p < 0.05$ was identified to be the significantly altered pathway (abbreviated as significant pathways).

Results

Metformin inhibits the proliferation of CCA cells in a dose-dependent manner

To address the anticancer effect of metformin on CCA, we conducted MTS assays and colony formation assays. Mz-ChA–1 cells were treated with various levels of metformin for both assays. MTS assays showed that metformin reduced cell viability in a dose-dependent manner (Figure 1A). Moreover, relative cell viabilities were significantly decreased to 80–90% when the cells were treated with 0.5 mM metformin. In colony formation assays, metformin at either 0.5 mM or 5 mM profoundly decreased the dimension of colonies (Figure 1B). Thus, 0.5 mM metformin was used to treat CCA cells in the following metabonomic analysis.

Metformin markedly changes the metabolic profile of CCA cells.

To reveal the metabolic distinction between the metformin-treated (Met) and control (Ctrl) groups, we performed NMR-based metabonomic analysis on aqueous extracts derived from CCA cells. The typical 1D ^{1}H NOEYS spectra and resonance assignments are shown in Figure 2 and Table S1, respectively. Totally, 43 metabolites were identified based on the NMR spectra.

Both PCA and PLS-DA were performed based on the normalized NMR data to evaluate the effect of metformin treatment on the metabolic profiles of CCA cells (Figure 3A & 3B). All the samples are situated in the Hotelling's T2 oval of the 95% confidence intervals. In the scores plot of either the PCA model or the PLS-DA model, each point represents a sample, and the distance between points reflects the degree of metabolic distinction. The PCA scores plot shows a distinct separation between Met and Ctrl groups, suggesting that metformin treatment markedly changed the metabolic profile of CCA cells (Figure 3A). The PLS-DA scores plot displays the improved metabolic separation between the two groups (Figure 3B). The cross-validation plot indicates the reliability of the PLS-DA model (Figure 3C).

Additionally, the HCA analysis was also conducted to confirm the validities of the PCA and PLS-DA models (Figure 3D). The dendrogram plot of HCA shows that the Met group forms a separate cluster, while the Ctrl group belongs to another cluster. This result well supported those from PCA and PLS-DA.

Metformin remarkably alters the levels of significant metabolites in CCA cells.

As showed in the loading plot of the PLS-DA model (Figure 3E), variables colored in red, yellow and blue are very significant, significant and insignificant, respectively. Moreover, the upward or downward direction indicates the variable was upregulated or downregulated in the Met group compared with the Ctrl group. Expectedly, the level of metformin was significantly increased in the Met group, indicating that extracellular metformin was transported into the cells. Besides, we identified 32 significant metabolites primarily responsible for the metabolic separation between the two groups. Compared with the Ctrl group, 14 metabolites were increased including pyruvate, lactate, glycerol, formate, NAD+, leucine, isoleucine, valine, methionine, lysine, phenylalanine, creatine, GPC and UDP-GlcNAc, while 18 metabolites were decreased including glucose, 2-oxoglutarate (α-KG) fumarate alanine, glutamine, glutamate, GABA, glycine, aspartate, asparagine, hydroxyproline, β-alanine, glutathione, taurine, creatine-P, PC, GTP, and myo-inositol.

Relative concentrations of metabolites were represented by relative integrals measured from 1D ^{1}H NOESY spectra. The quantitative comparison of relative concentrations of metabolites between the Met and Ctrl groups is showed in Table 1. Totally, 33 metabolites with statistical significance (p<0.05) were identified to be differential metabolites. The 14 increased differential metabolites were fully identical to

the 14 increased significant metabolites, while 19 decreased differential metabolites covered the 18 decreased significant metabolites except choline. Thus, choline was excluded from the further analysis, and the 32 significant metabolites also acted characteristic metabolites.

Metformin significantly alters metabolic pathways in CCA cells

By conducting metabolic pathway analysis based on the characteristic metabolites, we identified four significantly altered metabolic pathways, including glucose metabolism, oxidative stress-related metabolism, energy metabolism, and amino acids metabolism (Figure 4A). The relative concentrations of characteristic metabolites involved in the four significant pathways were quantitatively compared between the Met and Ctrl groups (Figure 4B, 4C and 4D). The levels of pyruvate, lactate and NAD+ were up-regulated in the metformin-treated cells, whereas the levels of glucose, GTP and TCA cycle intermediates (2-oxoglutarte; fumarate) were down-regulated. Furthermore, most of the detected non-essential amino acids were decreased, and some of the detected essential amino acids (methionine, phenylalanine, valine, leucine, and isoleucine) tended to be increased in the metformin-treated cells.

To visualize the effects of metformin treatment on metabolic in CCA cells, we projected the characteristic metabolites onto a metabolic map (Figure 5). Both the primarily changed characteristic metabolites and significantly altered metabolic pathways provide new insights into the molecular mechanisms underlying the anticancer effects of metformin on CCA cells.

Discussion

CCA is an aggressive malignancy which is well recognized as a highly metastatic cancer. CCA patients are mostly clinically silent and difficult to be diagnosed until the metastatic stage and often accompanied by low surgical resection rates, leading to a poor prognosis. As an oral anti-hyperglycemic drug from the biguanide family, Metformin is extensively prescribed for the management of type II diabetes. Numerous epidemiological data have shown that metformin usage was significantly associated with reduced incidence in diverse cancers [5–7]. Particularly, a recent epidemiological study including 1,828 potential CCA patients asserted that, metformin usage was significantly associated with 60% reduction in CCA risk in diabetic patients [27]. These data indicate that metformin has a potential value for CCA management and therapy.

In this study, we showed that metformin treatment had an anti-proliferation effect on CCA cell line Mz-ChA–1 in a dose-dependent manner. For further investigation, we conducted NMR-based metabonomic analysis to identify primarily changed metabolites and significantly altered metabolic pathways associated with the metformin treatment. We also performed univariate analysis to quantitatively compare metabolite levels between the Met and Ctrl groups of CCA cells. These results suggest that the

anticancer effect of metformin on CCA is closely related to glucose metabolism and amino acid metabolism.

It has been previously reported that metformin is transported into hepatocytes through the organic cation transporter (OTC) family [28]. Particularly, genetic variation in the OTC1 is well correlated to the therapeutic efficacy of metformin treatment [28]. In the present work, we have observed an accumulation of metformin in the Mz-ChA–1 cells, showing that metformin was transported into the cells and exhibited its effects.

Cancer cells rely on the input of glucose, amino acids, and fatty acids to maintain mitochondrial respiration and ATP production [29]. As the resultant product of glycolysis, pyruvate could be dehydrogenated to generate acetyl coenzyme A (CoA) which thereafter enters the TCA cycle. In this study, we observed an accumulation of pyruvate and significant reduction of TCA cycle intermediates including 2-oxoglutarte and fumarate in the Met group, suggesting that metformin treatment not only reduced the entry of pyruvate into TCA cycle, but also impaired the cycling of TCA intermediates. Our result well supports a recent published study exhibiting that metformin treatment greatly inhibited the biosynthesis of acetyl CoA, which was partly generated by pyruvate dehydrogenase complex (PDC) [30]. Moreover, various in vivo and in vitro studies have reported that metformin treatment could reduce the activity of mitochondrial complex I [12, 31] and cause the alterations in the electron transport chain (ETC). As a result, NADH-contained electrons are not effectively transported through the ETC, thus decreasing the NAD+ level [16, 32]. However, we observed that the NAD+ level was raised by metformin-treated CCA cells. Given the enhanced glucose consumption and lactate production, we assumed that metformin treatment boosted glycolysis and drained the electrons from NADH for the reduction of pyruvate to lactate. It is well known that the regulation of glycolysis is highly associated with AMPK, which can be activated by metformin [19, 33, 34]. Similarly, our data indicates that glycolysis is greatly affected by metformin, providing independent support for the viewpoint that AMPK is vital for the anticancer effect of metformin on CCA.

Amino acids play an irreplaceable role in the survival of cancer cells which have an increased requirement for these nutrients to support their aberrantly rapid proliferation rate. Besides acting as building blocks of protein, amino acids can function as metabolites and metabolic regulators in cancer cells [35, 36]. Certain amino acids contribute to flux into the TCA cycle via deamination and transamination reactions to generate TCA intermediates as an anaplerotic way. For example, glutamate can be transferred into mitochondria and converted to α-KG through oxidative deamination by glutamate dehydrogenase. Glutamate can also be transformed into α-KG in either cytoplasm or mitochondria by the action of several enzymes which transfer the amine from glutamate for use in alanine, aspartate, and serine biosynthetic reactions, or release the amine as free ammonia. Therefore, biosynthesis of amino acids is tightly linked to the TCA cycle and glutamate metabolism. Our data showed that the levels of glutamate, aspartate, asparagine, alanine, β-alanine, γ-aminobutyric acid (GABA) and ornithine were all decreased by metformin treatment, indicating that metformin has a significant effect on the synthesis of non-essential amino acids.

Due to the lack of substrates, glutathione was insufficient and thus interrupted the oxidative stress in metformin-treated cells. It is noteworthy that the taurine level was also significantly declined in the Met cells. As one of the most abundant amino acids, taurine is often acknowledged for its contribution to antioxidative effect [37, 38]. Depletion of taurine imply that metformin might cause oxidative stress in cells and increase the consumption of taurine as an alternative antioxidation source.

Furthermore, metformin treatment enhanced the levels of three branched chain amino acids (BCAAs) including leucine, isoleucine and valine. As essential amino acids, BCAAs cannot be synthesized endogenously and their catabolism shares two unique initial enzymatic steps: transamination of BCAAs that produces branched-chain α-keto acids (BCKA including KIC, KMV and KIV), oxidative decarboxylation of BCKAs [39]. However, our data showed that the levels of KMV, KIC were not significantly changed after metformin treatment, suggesting that metformin did not substantially disturb the substrate utilization in BCAA catabolism. Based on these results, we hypothesize that the accumulation of BCAAs and other essential amino acids might be due to the occurrence of autophagy that induces the degradation of protein. Previous works have well demonstrated that metformin could significantly contribute to the inhibition of mTOR [20, 21], directly leading to the activation of autophagy [40, 41]. Consistently with these works, our result provides independent support for the viewpoint that metformin may exert anticancer effect through activating the process of autophagy.

On the other hand, it was previously reported that metformin could induce cell cycle arrest in several other cancer cell lines [42–44]. Interestingly, we observed the significantly increased level of UDP-GlcNAc in metformin-treated Mz-ChA–1 cells. To our knowledge, this observation represents the first report that the anticancer effect of metformin is related to UDP-GlcNAc. As is known, UDP-GlcNAc is a common donor substrate for the N-glycosylation of most cell-surface receptors and transporters in eukaryotes [45]. Previous works indicated that glycoproteins with few N-glycans were significantly increased in a switch-like response to the enhanced UDP-GlcNAc level, such as TβR, CTLA–4 and GLUT4 which mediated organogenesis, differentiation and cell cycle arrest [46, 47]. Contrarily, glycoproteins with high numbers of N-glycans were slowly increased with the enhanced UDP-GlcNAc level, including EGFR, IGFR, FGFR, and PDGFR which stimulated growth and proliferation [46, 47]. Thus, UDP-GlcNAc with an enhanced level in Mz-ChA–1 cells could potentially increase surface levels of low-n glycoproteins, and eventually drive to arrest programs and suppress proliferation. Further work should be conducted in the future to mechanistically understand the relevance between metformin and cell cycle arrest.

Conclusion

In this work, we have carried out a comprehensive NMR-based metabolomic analysis to access the anticancer effect of metformin on CCA cells and address the underlying molecular mechanisms. By a combination of ^{1}H NMR detection, multivariate statistical analysis, metabolite quantification and metabolic pathway analysis, we found that metformin treatment induced significant metabolic alterations, such as boosting glycolysis, down-regulating the TCA cycle and causing a lack of non-essential amino acids. Moreover, the accumulation of essential amino acids suggests that metformin

treatment might activate the process of autophagy. Furthermore, the increased level of UDP-GlcNAc highlights the relevance between metformin and cell cycle arrest. These results extend our understanding on the molecular mechanisms underlying the anticancer effect of metformin on CCA, and shed light on the clinical use of metformin for CCA managements.

Abbreviations

CCA: Cholangiocarcinoma

PCA: principal component analysis

PLS-DA: Partial Least Squares-Discriminant Analysis

OPLS-DA: Orthogonal Partial Least Squares-Discriminant Analysis

VIP: variable importance in the projection

KEGG: Kyoto Encyclopedia of Genes and Genomes

BCAA: Branched Chain Amino Acid

GABA: 4-Amino Butyric Acid

PC: O = Phosphocholine

GPC: sn-Glycero–3-Phosphocholine

Creatine-P: Creatine-Phosphate

NAD: Nicotinamide Adenine Dinucleotide

NAAD: Nicotinic Acid Adenine Dinucleotide

UDP-GlcNAc: UDP-N-acetylglucosamine

KMVA: 3-methyl–2-oxovalerate

GTP/PPPi: Guanosine triphosphate

Acetyl CoA: Acetyl Coenzyme A

TCA cycle: Tricarboxylic Acid Cycle

Declarations

Ethics approval and consent to participate

No applicable

Consent to publish

No applicable

Availability of data and materials

The datasets generated and analyzed during the current study are not publicly available due to no available and appropriate public database can be achieved, but are available from the corresponding author on reasonable request.

Competing interests

The authors declare that they have no competing interests.

Funding

This work is sponsored by a. The national science and technology major project of china (2017ZX10203206 to W.L) b. Scientific research foundation for advanced talents, xiang' an hospital of Xiamen university(NO.PM20180917008 to W.L)

Authors' Contributions

Jin Zhang established the cell models, conducted the NMR detection and interpreted the metabonomic data and was the main writer for this manuscript. Caihua Hang and Wei Shao provided certain help on NMR analysis and cell culturing. Wengang Li was the initiator of this study. Donghai Lin is the ultimate checker for this manuscript. All authors have read and approved the final version of this manuscript.

Acknowledgements

None.

References

1.Rizvi, S. and G. J. Gores, *Pathogenesis, diagnosis, and management of cholangiocarcinoma.* Gastroenterology, 2013. *145(*6): p. 1215–29.

2.Razumilava, N. and G. J. Gores, *Cholangiocarcinoma.* Lancet, 2014. *383(*9935): p. 2168–79.

3.Doherty, B., V. E. Nambudiri, and W. C. Palmer, *Update on the Diagnosis and Treatment of Cholangiocarcinoma.* Curr Gastroenterol Rep, 2017. *19(*1): p. 2.

4.Brito, A. F., et al., *Cholangiocarcinoma: from molecular biology to treatment.* Med Oncol, 2015. *32(*11): p. 245.

5.Tseng, C. H., *Metformin and endometrial cancer risk in Chinese women with type 2 diabetes mellitus in Taiwan.* Gynecol Oncol, 2015.

6.Evans, J. M. M., et al., *Metformin and reduced risk of cancer in diabetic patients.* British Medical Journal, 2005. *330(*7503): p. 1304–1305.

7.DeCensi, A., et al., *Metformin and Cancer Risk in Diabetic Patients: A Systematic Review and Meta-analysis.* Cancer Prevention Research, 2010. *3(*11): p. 1451–1461.

8.Zhang, Z. J., et al., *Reduced Risk of Lung Cancer With Metformin Therapy in Diabetic Patients: A Systematic Review and Meta-Analysis.* American Journal of Epidemiology, 2014. *180(*1): p. 11–14.

9.Schuler, K. M., et al., *Antiproliferative and metabolic effects of metformin in a preoperative window clinical trial for endometrial cancer.* Cancer Medicine, 2015. *4(*2): p. 161–173.

10.Alimova, I. N., et al., *Metformin inhibits breast cancer cell growth, colony formation and induces cell cycle arrest in vitro.* Cell Cycle, 2009. *8(*6): p. 909–915.

11.Ling, S., et al., *Metformin inhibits proliferation and enhances chemosensitivity of intrahepatic cholangiocarcinoma cell lines.* Oncol Rep, 2014. *31(*6): p. 2611–8.

12.Saengboonmee, C., et al., *Metformin Exerts Antiproliferative and Anti-metastatic Effects Against Cholangiocarcinoma Cells by Targeting STAT3 and NF-kB.* Anticancer Res, 2017. *37(*1): p. 115–123.

13.Jiang, X. M., et al., *Metformin inhibits tumor growth by regulating multiple miRNAs in human cholangiocarcinoma.* Oncotarget, 2015. *6(*5): p. 3178–3194.

14.Lord, S. R., et al., *Integrated Pharmacodynamic Analysis Identifies Two Metabolic Adaption Pathways to Metformin in Breast Cancer.* Cell metabolism, 2018. *28(*5).

15.Wheaton, W. W., et al., *Metformin inhibits mitochondrial complex I of cancer cells to reduce tumorigenesis.* Elife, 2014. *3:* p. e02242.

16.*Metformin and phenformin deplete tricarboxylic acid cycle and glycolytic intermediates during cell transformation and NTPs in cancer stem cells.*

17.Shi, W. Y., et al., *Therapeutic metformin/AMPK activation blocked lymphoma cell growth via inhibition of mTOR pathway and induction of autophagy.* Cell Death Dis, 2012. *3:* p. e275.

18.Zakikhani, M., et al., *Metformin is an AMP kinase-dependent growth inhibitor for breast cancer cells.* Cancer Res, 2006. *66(*21): p. 10269–73.

19.Zhang, C. S., et al., *Metformin Activates AMPK through the Lysosomal Pathway.* Cell Metab, 2016. *24(*4): p. 521–522.

20.Gwinn, D. M., et al., *AMPK phosphorylation of raptor mediates a metabolic checkpoint.* Mol Cell, 2008. *30(*2): p. 214–26.

21.Wu, L., et al., *An Ancient, Unified Mechanism for Metformin Growth Inhibition in C. elegans and Cancer.* Cell, 2016. *167(*7): p. 1705–1718.e13.

22.Morvan, D., *Functional metabolomics uncovers metabolic alterations associated to severe oxidative stress in MCF7 breast cancer cells exposed to ascididemin.* Mar Drugs, 2013. *11(*10): p. 3846–60.

23.Liu, X., et al., *LC-based targeted metabolomics analysis of nucleotides and identification of biomarkers associated with chemotherapeutic drugs in cultured cell models.* Anticancer Drugs, 2014. *25(*6): p. 690–703.

24.Li, Y., et al., *The antitumor effect of formosanin C on HepG2 cell as revealed by 1H-NMR based metabolic profiling.* Chem Biol Interact, 2014. *220:* p. 193–9.

25.Knuth, A., et al., *Biliary adenocarcinoma. Characterisation of three new human tumor cell lines.* J Hepatol, 1985. *1(*6): p. 579–96.

26.Xia, J. and D. S. Wishart, *MSEA: a web-based tool to identify biologically meaningful patterns in quantitative metabolomic data.* Nucleic Acids Res, 2010. *38(*Web Server issue): p. W71–7.

27.Chaiteerakij, R., et al., *Risk Factors for Intrahepatic Cholangiocarcinoma: Association Between Metformin Use and Reduced Cancer Risk.* Hepatology, 2013. *57(*2): p. 648–655.

28.Shu, Y., et al., *Effect of genetic variation in the organic cation transporter 1 (OCT1) on metformin action.* The Journal of Clinical Investigation, 2007. *117(*5): p. 1422–1431.

29.Sciacovelli, M., et al., *The metabolic alterations of cancer cells.* Methods Enzymol, 2014. *542:* p. 1–23.

30.Cuyas, E., et al., *Metformin targets histone acetylation in cancer-prone epithelial cells.* Cell cycle (Georgetown, Tex.), 2016. *15(*24): p. 3355–3361.

31.Pryor, R. and F. Cabreiro, *Repurposing metformin: an old drug with new tricks in its binding pockets.* The Biochemical journal, 2015. *471(*3): p. 307–22.

32.Griss, T., et al., *Metformin Antagonizes Cancer Cell Proliferation by Suppressing Mitochondrial-Dependent Biosynthesis.* Plos Biology, 2015. *13(*12).

33.Stephenne, X., et al., *Metformin activates AMP-activated protein kinase in primary human hepatocytes by decreasing cellular energy status.* Diabetologia, 2011. *54(*12): p. 3101–10.

34.Meng, S., et al., *Metformin activates AMP-activated protein kinase by promoting formation of the alphabetagamma heterotrimeric complex.* J Biol Chem, 2015. *290(*6): p. 3793–802.

35.Tsun, Z. Y. and R. Possemato, *Amino acid management in cancer.* Semin Cell Dev Biol, 2015. *43:* p. 22–32.

36.Li, Z. and H. Zhang, *Reprogramming of glucose, fatty acid and amino acid metabolism for cancer progression.* Cellular and Molecular Life Sciences, 2016. *73(*2): p. 377–392.

37.Lambert, I. H., et al., *Physiological role of taurine—from organism to organelle.* Acta Physiol (Oxf), 2015. *213(*1): p. 191–212.

38.Aly, H. A. A. and R. M. Khafagy, *Taurine reverses endosulfan-induced oxidative stress and apoptosis in adult rat testis.* Food and Chemical Toxicology, 2014. *64(*Supplement C): p. 1–9.

39.Hutson, S. M., A. J. Sweatt, and K. F. Lanoue, *Branched-chain amino acid metabolism: implications for establishing safe intakes.* J Nutr, 2005. *135(*6 Suppl): p. 1557s–64s.

40.Melendez, A., et al., *Autophagy genes are essential for dauer development and life-span extension in C. elegans.* Science, 2003. *301(*5638): p. 1387–91.

41.Madeo, F., et al., *Caloric restriction mimetics: towards a molecular definition.* Nat Rev Drug Discov, 2014. *13(*10): p. 727–40.

42.Queiroz, E. A., et al., *Metformin induces apoptosis and cell cycle arrest mediated by oxidative stress, AMPK and FOXO3a in MCF–7 breast cancer cells.* PLoS One, 2014. *9(*5): p. e98207.

43.Cai, X., et al., *Metformin Induced AMPK Activation, G0/G1 Phase Cell Cycle Arrest and the Inhibition of Growth of Esophageal Squamous Cell Carcinomas In Vitro and In Vivo.* PLoS One, 2015. *10(7*): p. e0133349.

44.Jeong, Y. K., et al., *Metformin Radiosensitizes p53-Deficient Colorectal Cancer Cells through Induction of G2/M Arrest and Inhibition of DNA Repair Proteins.* PLoS One, 2015. *10(*11): p. e0143596.

45.Mkhikian, H., et al., *Golgi self-correction generates bioequivalent glycans to preserve cellular homeostasis.* eLife, 2016. *5:* p. e14814.

46.Dennis, J. W., I. R. Nabi, and M. Demetriou, *Metabolism, Cell Surface Organization, and Disease.* Cell, 2009. *139(7*): p. 1229–1241.

47.Lau, K. S., et al., *Complex N-glycan number and degree of branching cooperate to regulate cell proliferation and differentiation.* Cell, 2007. *129(*1): p. 123–34.

Table

Table 1. Quantitative comparison of metabolite levels between the Met and Ctrl groups based on relative integrals calculated from the 1D ^{1}H-NMR spectra.

Metabolite	Mean ± SD		Significance	*p* value
	Ctrl	Met		
2-oxoglutarate	1.000 ± 0.114	0.590 ± 0.052	***	< 0.001
KIC	1.000 ± 0.121	0.903 ± 0.081	NS	0.136
KMV	1.000 ± 0.146	0.856 ± 0.131	NS	0.104
GABA	1.000 ± 0.034	0.841 ± 0.085	**	0.002
acetate	1.000 ± 0.262	0.804 ± 0.186	NS	0.166
alanine	1.000 ± 0.073	0.716 ± 0.044	***	< 0.001
asparagine	1.000 ± 0.076	0.749 ± 0.051	***	< 0.001
aspartate	1.000 ± 0.133	0.677 ± 0.090	***	0.001
β-alanine	1.000 ± 0.097	0.517 ± 0.041	***	< 0.001
choline	1.000 ± 0.072	1.192 ± 0.084	**	0.002
creatine	1.000 ± 0.120	0.752 ± 0.065	**	0.001
creatine-P	1.000 ± 0.042	0.729 ± 0.186	**	0.006
formate	1.000 ± 0.173	1.429 ± 0.357	*	0.024
fumarate	1.000 ± 0.034	0.333 ± 0.070	***	< 0.001
glucose	1.000 ± 0.426	0.473 ± 0.210	*	0.022
glutamate	1.000 ± 0.049	0.669 ± 0.043	***	< 0.001
glutamine	1.000 ± 0.066	0.694 ± 0.219	**	0.008
glutathione	1.000 ± 0.251	0.459 ± 0.158	**	0.001
glycerol	1.000 ± 0.063	1.504 ± 0.106	***	< 0.001
glycine	1.000 ± 0.053	0.847 ± 0.047	***	0.000
GTP	1.000 ± 0.056	0.869 ± 0.035	***	0.001
histidine	1.000 ± 0.051	0.925 ± 0.084	NS	0.092
hydroxyproline	1.000 ± 0.062	0.603 ± 0.071	***	< 0.001
isoleucine	1.000 ± 0.052	1.342 ± 0.088	***	< 0.001
lactate	1.000 ± 0.088	1.325 ± 0.069	***	< 0.001
leucine	1.000 ± 0.061	1.382 ± 0.082	***	< 0.001
lysine	1.000 ± 0.067	1.209 ± 0.023	***	< 0.001
methionine	1.000 ± 0.038	1.339 ± 0.070	***	< 0.001
myo-inositol	1.000 ± 0.038	0.663 ± 0.037	***	< 0.001
NAD+	1.000 ± 0.043	1.091 ± 0.051	**	0.008
PC	1.000 ± 0.189	0.609 ± 0.115	**	0.002
ornithine	1.000 ± 0.071	0.974 ± 0.052	NS	0.478
phenylalanine	1.000 ± 0.047	1.193 ± 0.074	***	0.000
proline	1.000 ± 0.089	0.911 ± 0.045	NS	0.055
putrescine	1.000 ± 0.137	1.119 ± 0.109	NS	0.128
pyruvate	1.000 ± 0.115	1.349 ± 0.278	*	0.017
serine	1.000 ± 0.092	1.023 ± 0.049	NS	0.597
GPC	1.000 ± 0.053	1.264 ± 0.020	***	< 0.001
taurine	1.000 ± 0.036	0.609 ± 0.053	***	< 0.001
tyrosine	1.000 ± 0.046	1.037 ± 0.081	NS	0.354

UDP-GlcNAc	1.000 ± 0.039	1.731 ± 0.190	***	< 0.001
valine	1.000 ± 0.076	1.486 ± 0.085	***	< 0.001

Symbols ***, **, *, NS indicate differences between the Met and Ctrl groups were highly significant ($p<0.001$), very significant ($p<0.01$), significant ($p<0.05$), insignificant ($p\geq0.05$) respectively. Red or blue color denotes that the metabolite level was elevated or reduced in the metformin-treated cells relative to control cells.

Figures

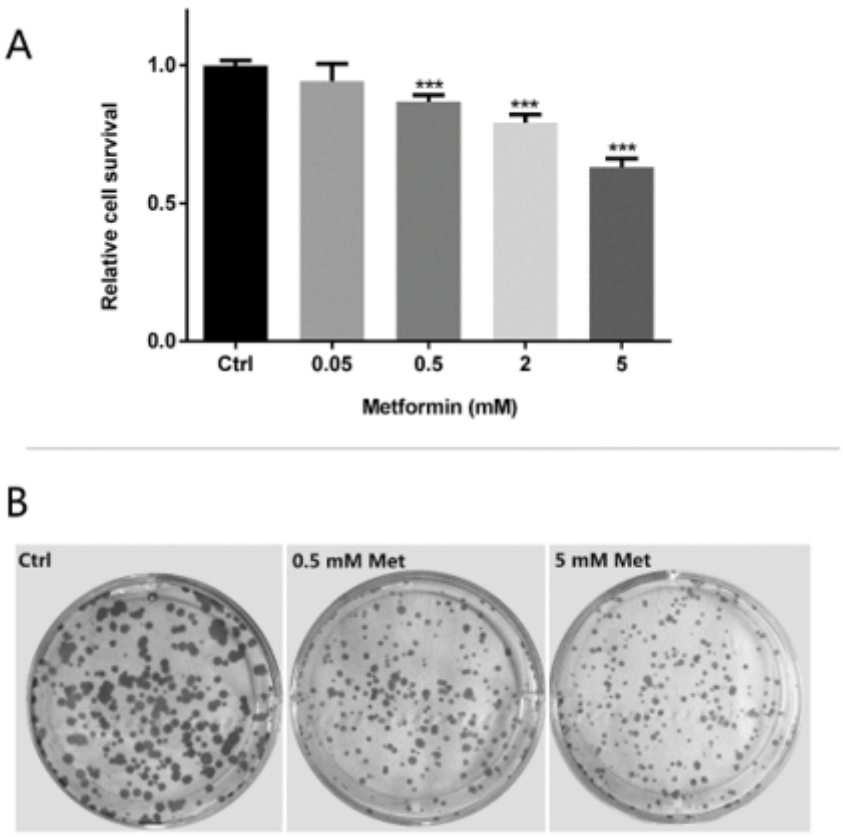

Figure 1

Metformin inhibited the proliferation of Mz-ChA-1 cells in a dose-dependent manner. (A) Relative cell viabilities when the cells were treated with various concentrations of metformin. n=10, *** $p < 0.001$ relative to control cells. (B) Colony formation of the cells before and after metformin treatment.

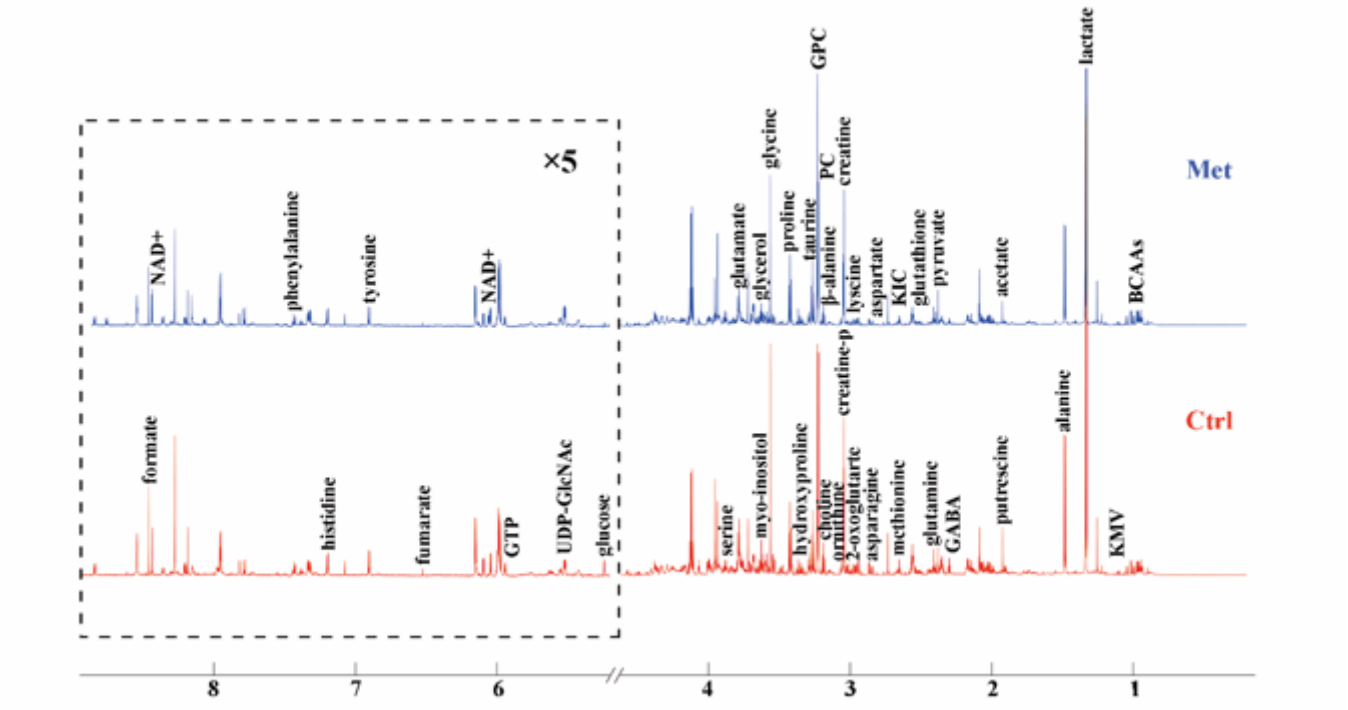

Figure 2

Averaged 1D 1H NOESY spectra of aqueous metabolites derived from the metformin-treated (Met) and control (Ctrl) groups of Mz-ChA-1 cells. Spectral regions of 1.0-4.6 ppm and 5.2-9.0 ppm were reserved, and the water region (4.6–5.2 ppm) was removed. Spectral regions of 5.2-9.0 ppm were scaled for 5 times. Assigned resonances are labeled in the spectra. BCCAs: branched chain amino acids (valine, leucine and isoleucine); KMV: 3-methyl-2-oxovalerate; KIC: 2-oxoisocaproate; GABA: 4-aminobutyrate; creatine-P: creatine phosphate; PC: O-phosphocholine; GPC: sn-glycero-3-phosphocholine.

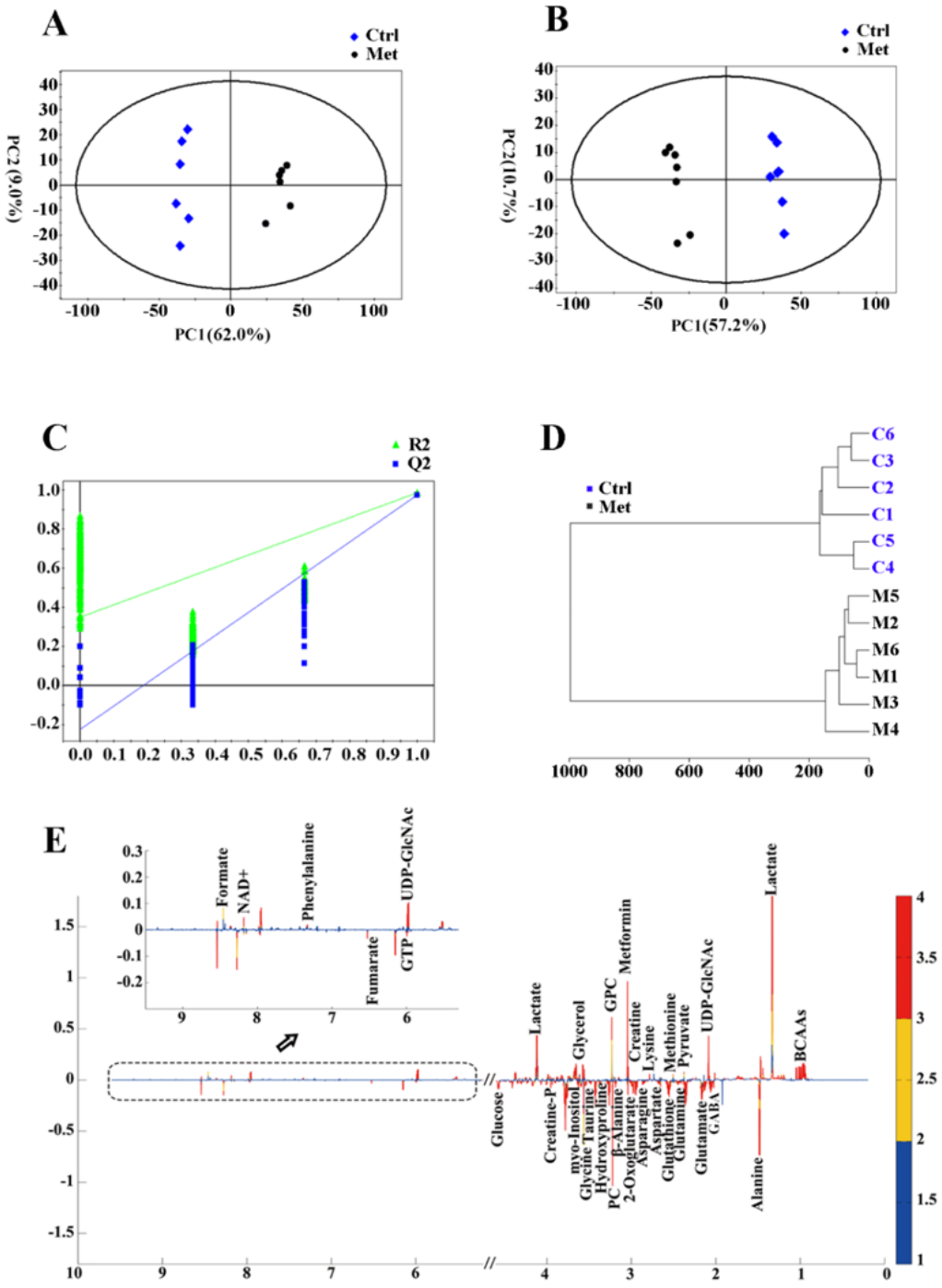

Figure 3

Multivariate statistical analysis of NMR spectral data of aqueous extracts derived from the Met and Ctrl groups of Mz-ChA-1 cells. (A) PCA scores plot; (B) PLS-DA scores plot; (C) PLS-DA cross-validation plot; (D) Hierarchical cluster plot (E) PLS-DA loading plot for identifying significant metabolites primarily contributing to the metabolic discrimination between the two groups of cells.

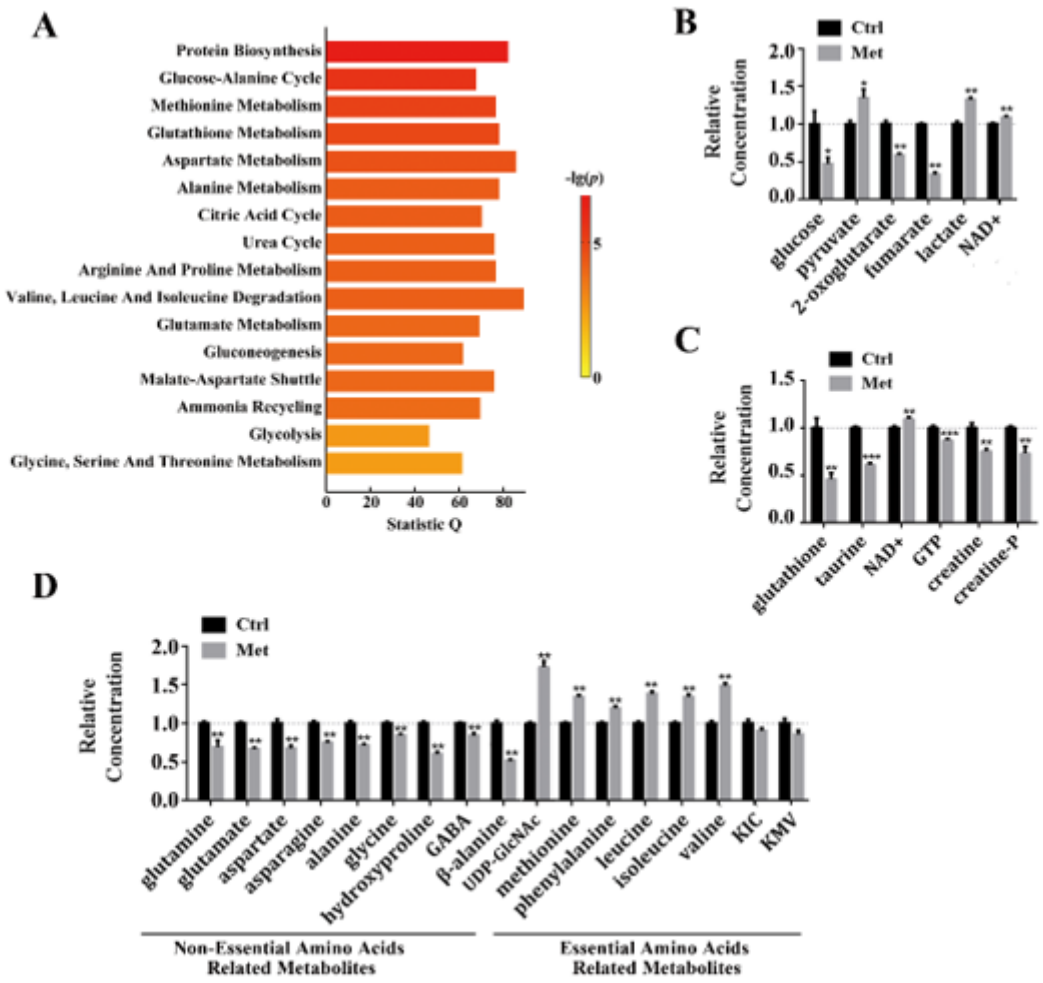

Figure 4

Altered metabolic pathways and changed metabolites in the Met group relative to the Ctrl group. (A) Significantly altered metabolic pathways identified from metabolite sets enrichment analysis based on characteristic metabolites. (B-D) Significantly changed metabolites related to glucose metabolism (B), energy metabolism and oxidative stress-related metabolism (C), and amino acids metabolism (D).

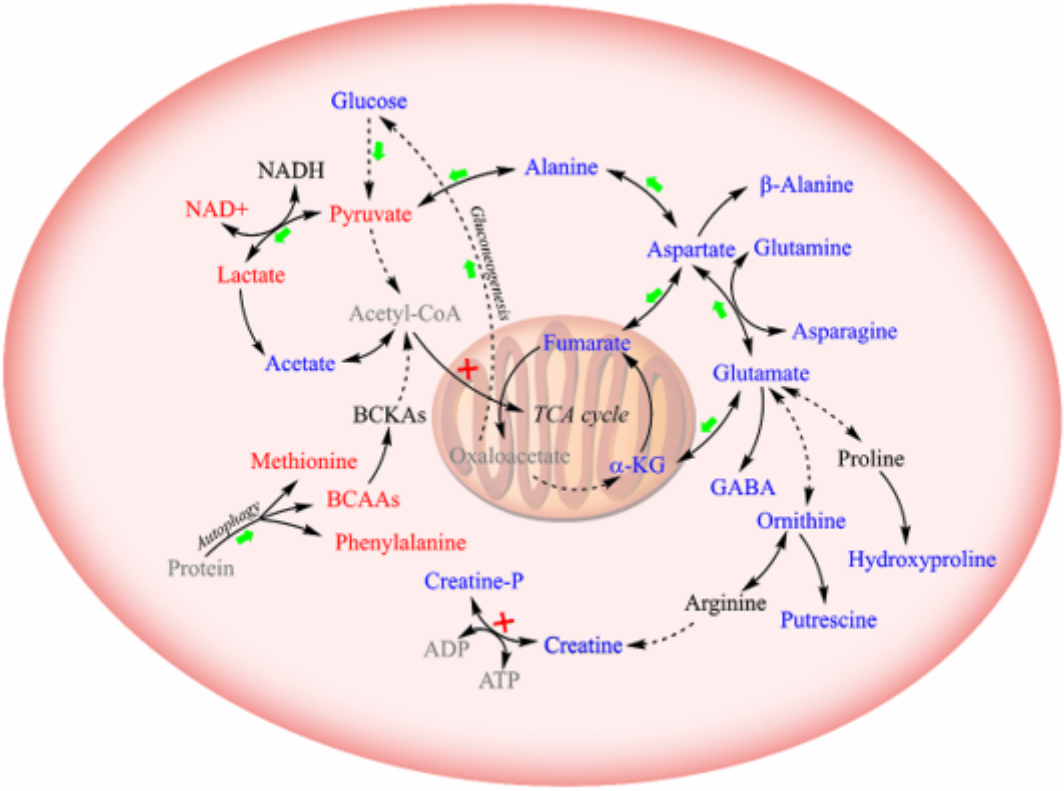

Figure 5

Schematic diagram for the effects of metformin treatment on metabolic pathways in cholangiocarcinoma Mz-ChA-1 cells. Solid lines: direct conversion; dotted line: indirect conversion. Metabolites colored in red, blue and black represent increased, decreased and unchanged levels in metformin-treated cells relative to control cells, respectively. Metabolites displayed in grey were not detected by 1H-NMR. Green arrows and red crosses denote potentially promoted and inhibited metabolic pathways in metformin-treated cells, respectively.

Supplementary Files

This is a list of supplementary files associated with this preprint. Click to download.

- Supplementarymaterials20191220.docx